Chapter 6

Surface Modification of Silicone Rubber by Ion Implantation to Improve Biocompatibility

Xin Zhou, Yiming Zhang, Xiaohua Shi and Dongli Fan

Additional information is available at the end of the chapter

http://dx.doi.org/10.5772/intechopen.68298

Abstract

Silicone Rubber (SR) and SR-based materials have been used as medical tissue implants in the field of plastic surgery for many years, but there are still some reports of adverse reactions to long-term implants. In our study, three types of carbon ion silicone rubber were obtained by implanting three doses of carbon ions. Then, the surface characteristics, the antibacterial adhesion properties and in vivo host responses were evaluated. These study shown that ion implantation change the surface roughness and zeta potential of virgin SR; it also inhibit bacterial adhesion. At the same time, ion implantation enhance the cell proliferation, adhesion and tissue compatibility. These data indicate that carbon ion implanted silicone rubber exhibits good antibacterial adhesion properties, cytocompatibility and triggers thinner and weaker tissue capsules. In addition, according to the surface characteristics, we speculate that high surface roughness and high zeta potential may be the main factors that induce the unique biocompatibility of carbon ion implanted silicone rubber. In this chapter, we will review these results above and propose that ion implantation should be considered for further investigation and application, and carbon ion silicone rubber could be a better biomaterial to decrease silicone rubber–initiated complications.

Keywords: ion implantation, silicone rubber, surface modification, biocompatibility

1. Introduction

Silicone rubber (SR) is a type of biomaterial that exhibits many useful properties, such as thermal stability, chemical resistance, and low cost [1]. It has a long history of use in biomedical

and biological applications, ranging from tissue fillers to tubes for dialysis and blood pumps [2–4]. Silicone rubber and silicone rubber-based materials have been used as medical tissue implants in the field of plastic surgery for many years, but there remain reports of adverse reactions to long-term implants, such as capsular contracture [5, 6]. Moreover, various prosthetic materials that contain silicone rubber can easily move and can permanently damage the prostheses. In addition, certain materials made from silicone rubber, such as catheters, are widely used in medicine but have several limitations; for example, bacteria can readily colonize the surfaces of silicone rubber, facilitating infection and even causing patient death in certain cases [5, 7–9].

In recent years, many attempts have been made to modify medical materials to reduce bacterial adhesion and to minimize adverse inflammatory or foreign body reactions [10–15]. Among these methods, the surface modification of biomaterials is an economical and effective method to achieve biocompatibility and biofunctionality while preserving the favorable characteristics of the biomaterial, such as particular mechanical properties and thermal stability. Surface modifications, such as ion implantation [16–18], sintering [19], electrochemical deposition [20], and the sol-gel coating method, are common [21]. Among these surface modification methods, ion implantation has become a notably useful method because of its ease of operation and convenience [22–25]. In this context, we implanted three different doses of carbon ions into silicone rubber and obtained carbon ion silicone rubber (C-SR). Our study was designed to evaluate the surface characteristics and the biocompatibility of carbon ion silicone rubber. We focused on bacterial adhesion, cytocompatibility, and fibrosis/fibrous capsule development. The long-term goal is to gain a better biomaterial for use by plastic surgeons.

2. Materials and methods

2.1. Sample preparation

SR sheets with dimensions of 100 x 100 x 1 mm were prepared from a two-component silicone system. Both component A and component B were clinical-quality liquids provided by Chenguang Research Institute of Chemical Engineering, China. Three doses of carbon ions were implanted using the ion implanter, respectively. The doses are 1×10^{15} ions/cm^2 (C1), 3×10^{15} ions/cm^2 (C2), and 1×10^{16} ions/cm^2 (C3). After that, SR and C-SR sheets were manufactured into disc-like samples with a diameter of 6 mm using a hole puncher and into square samples with dimensions of 10 mm × 10 mm × 1 mm. The disc-like samples were used in in vitro antibacterial adhesion tests, and the square samples were used for in vivo evaluation. All samples were sterilized with 75% alcohol overnight. In all experiments, SR served as the control.

2.2. Surface characterization

The mechanical properties were analyzed by shore A durometer and electronic universal testing machine to gain parameters of the shore hardness and tear strength. The physicochemical properties were analyzed by the FTIR, SEM, XRD, XPS, water contract angel, zeta potential, and AFM experiments. The surface zeta potentials of materials were measured with a Zeta

Potential Analyzer (DelsaNano C, Beckman Coulter, Germany). The measurements were carried out in 1 mmol 1-L NaCl electrolyte solution and with standard particles for flat surface cell (Otsuka Electronic Co., Ltd, Japan). Each sample chooses five points and each point tests 20 times. After that, the samples were scanned by the Environment Control Scanning Probe Microscope (NanoNavi E-Sweep, NSK Ltd., Tokyo, Japan) and each sample was imaged with a 5 μm × 5 μm scanned area. The surfaces were analyzed by measuring the average surface roughness (Ra) of 5 randomly chosen images per sample from selected areas of 1 μm x 1 μm under Atomic Force Microscope (AFM) analysis software (NanoNavi II, SII Nano Technology Inc., Tokyo, Japan). Ra is defined as the average absolute deviation of the roughness irregularities from the mean line over one sampling length and gives a good general description of height variations. Three replicas were used.

2.3. Bacterial culture preparation

Gram-negative *Escherichia coli* (ATCC 25922), Gram-positive *Staphylococcus aureus* (ATCC 25923), and *S. epidermidis* (ATCC 12228) were employed to bacterial experiments. The strains were streaked on blood agar plates from frozen stocks and grown for 24 h at 37°C in ambient air. The agar plates were then kept at 4°C until further use. For each experiment, one colony from an agar plate was inoculated into 10 ml of tryptone soy broth (TSB) and incubated for 24 h. The bacterial suspension was then added to 0.9% sterile sodium chloride to a final concentration of 1.5 x 10^6 colony-forming units per ml (CFU/ml), after which a McFarland standard was prepared (in practical terms, OD600 nm = 0.132). The samples were placed on 96-well culture plates and separately incubated in 200 μl of the bacterial suspension at 37°C for 1 or 24 h. After that, the plate colony-counting, fluorescence staining, and scanning electron microscopy (SEM) observation were conducted.

2.3.1. Plate colony-counting

After incubation of the samples in the bacterial culture for 1 and 24 h, the bacteria on each sample were gently rinsed with PBS, respectively, and ultrasonically detached in 1 ml of PBS solution. The bacteria in the PBS were recultivated on agar plates for colony-counting. The antibacterial rates were determined based on the following relationship: antibacterial rate (%) = (CFU of control − CFU of experimental groups)/CFU of control x 100%. This assay was performed in triplicate.

2.3.2. Fluorescence staining

After incubation for 1 and 24 h, various samples were gently rinsed with PBS before staining the bacteria on the samples. The staining was performed by applying LIVE/DEAD® BacLight™ Bacterial Viability Kit (L7029, Molecular Probes®, OR, USA) for 15 min in darkness and was examined by laser scanning confocal microscopy (LEICA TCS SP5, Germany). The areas of green and red color in the pictures were then analyzed by using Image-Pro Plus version 6.0 (Media Cybernetics, Inc., USA) and then the proportion of red coloration based on the following relationship was calculated: red proportion (%) = red area/(green area + red area) x 100%.

2.3.3. Scanning electron microscopy (SEM) observation

After bacterial incubation for 1 and 24 h, the samples were rinsed with PBS to remove free bacterial cells and then fixed in 2.5% glutaraldehyde for 3 h at room temperature. The samples were then progressively dehydrated in a series of ethanol solutions (15, 30, 50, 70, 80, 90, 95, and 100%) for 15 min each. After that, the specimens underwent critical point drying and coating with a thin conductive layer of Au. Finally, the morphology and adhesion of the bacteria on the various samples were determined by SEM (VEGA 2 SEM, TESCAN Inc., Brno, Czech Republic).

2.4. Animals and surgery

This research was performed in accordance with the Guide for the Care and Use of Laboratory Animals published by the US National Institutes of Health (Washington, DC: The National Academies Press, 2011), and all of the animal protocols were approved by the Institutional Animal Care and Use Committee of the Third Military Medical University, China. A total of 16 female Sprague-Dawley rats (weighing 160–200 g) were used (4 groups of 4 animals each), and all rats were housed under a 12-h light–dark cycle with free access to water and food. Prior to surgery, all of the rats were anesthetized with 3% pentobarbital sodium (1 ml/1000 g). The skin was swabbed with iodine, and four parallel incisions (10 mm) were performed. The material samples were implanted subcutaneously along the back region. The implants and their surrounding tissues were retrieved from each group by wide excision at 7, 30, 90, and 180 days after implantation and were then fixed in 4% paraformaldehyde solution. After that, HE and Masson's staining and immunohistochemistry were carried out.

2.4.1. HE and Masson's staining

The fixed tissues were sectioned (6 μm thick) and stained using a HE Staining Kit (C0105, Beyotime Inc., Shanghai, China). The thickness of the fibrotic capsule around each implant was determined at five equidistant points for statistical accuracy. Collagen deposition in the tissue around the implants was studied by Masson's trichrome staining, which was performed using a staining kit (MST-8003, Maixin Biological Technology Co., Ltd., Fujian, China). All procedures were performed based on the manufacturer's instructions.

2.4.2. Immunohistochemistry

Immunohistochemistry was performed on 4% paraformaldehyde-fixed cryostat sections of frozen tissue specimens. Endogenous peroxidase and nonspecific antibody binding were blocked with 3% H_2O_2 and 100% methanol, with a ratio of 1:5 and a blocking time of 30 min. Next, 0.02 M PBS was used for antigen retrieval while heating in a water bath, followed by treatment with 5% blocking reagent at 37°C for 30 min. The slides were then incubated at 4°C for 12 h with a primary antibody against CD68, CD4, TNF-α, α-SMA, or elastin (1:25) (Boster Biological Engineering Co., Ltd., Hubei, China). After washing in PBS, a secondary antibody was applied for 30 min. Visualization was achieved by adding 3, 3′-diaminobenzidine chromogen.

2.5. Statistics

All data are expressed as the mean ± standard deviation (SD), and statistics were analyzed using SPSS statistical software. One-way ANOVA combined with multiple comparisons performed along with Tukey multiple comparison tests was utilized to determine the level of significance. In all of the statistical evaluations, $P < 0.05$ was considered significant.

3. Results

3.1. Ion implantation changes the surface roughness and zeta potential of SR

After ion implantation, SEM, AFM, FTIR, XPS, XRD, water contact angle measure instrument, zeta potential detection instrument, shore A durometer, and an electronic universal testing machine were used to investigate the change in properties of carbon ion silicone rubber. The SEM results failed to find any significant differences between virgin SR and three C-SRs (**Figure 1**), indicating that carbon ion implantation did not change the macroscale surface of SR.

At the same time, there is no any significant differences or the difference was very small on the results of FTIR (**Figure 2**), XRD (**Figure 3**), shore hardness (**Figure 4A**), and tear strength (**Figure 4B**).

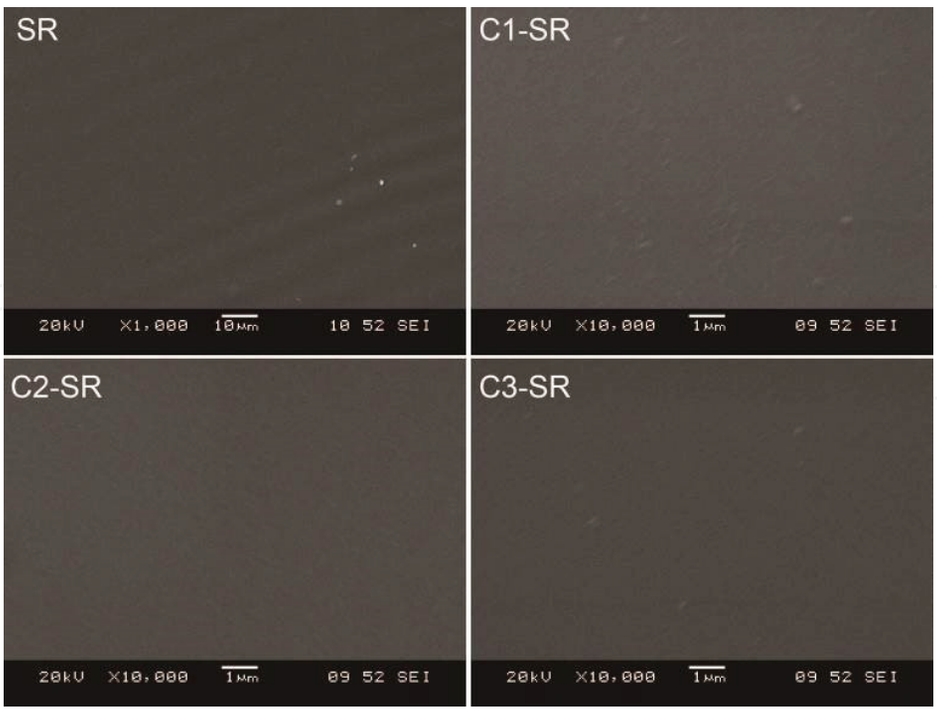

Figure 1. Representative scanning electron microscopic images of virgin silicone rubber and carbon ion-implanted silicone rubber.

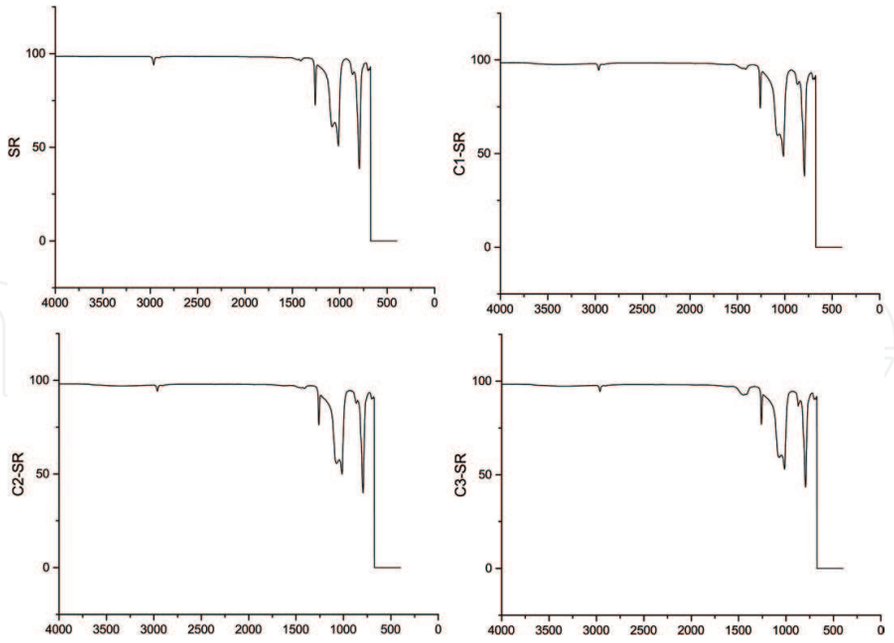

Figure 2. The Fourier transform infrared spectroscopy results of virgin silicone rubber and carbon ion-implanted silicone rubber.

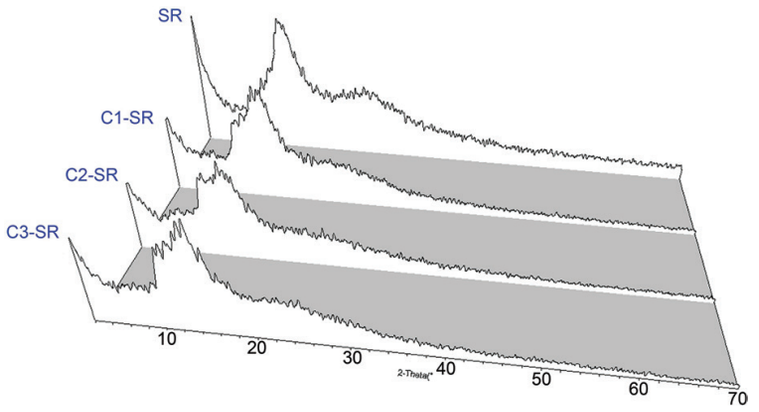

Figure 3. The XRD results of virgin silicone rubber and carbon ion-implanted silicone rubber.

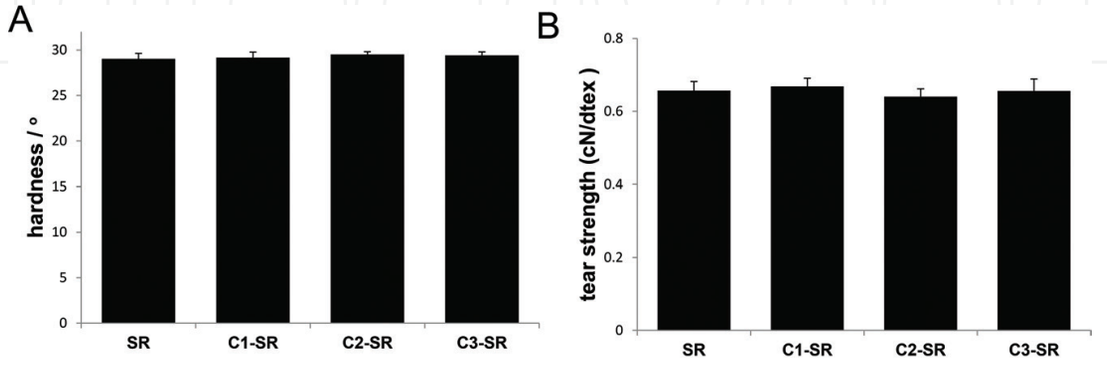

Figure 4. The results of Shore A hardness and tear strength of virgin silicone rubber and carbon ion-implanted silicone rubber. A, Shore A hardness. B, Tear strength.

From the results of water contact angle, we found that carbon ion implantation significantly decreased the water contact angle of SR, and big doses carbon ions had lowest water contact angle among all C-SRs (**Figure 5**).

Besides, the XPS results showed that carbon ion implantation significantly changed the surface silicone oxygen rate and chemical-element distribution of SR (**Figure 6**) (**Table 1**); we noted

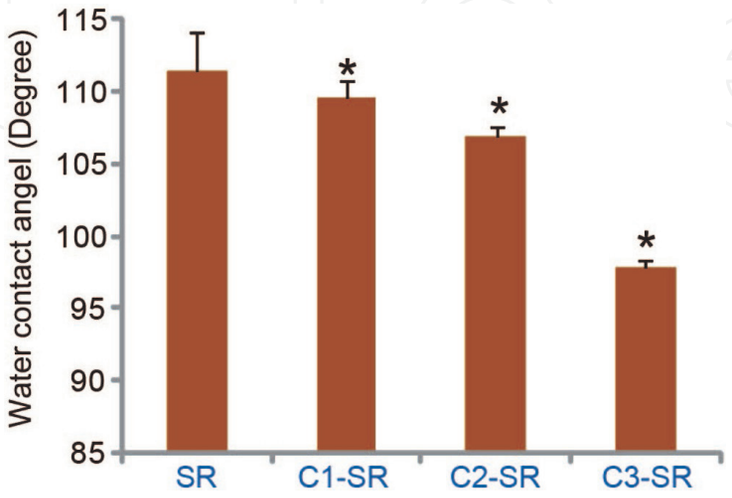

Figure 5. Water contact angle of virgin silicone rubber and carbon ion-implanted silicone rubber (*P < 0.05 compared with silicone rubber).

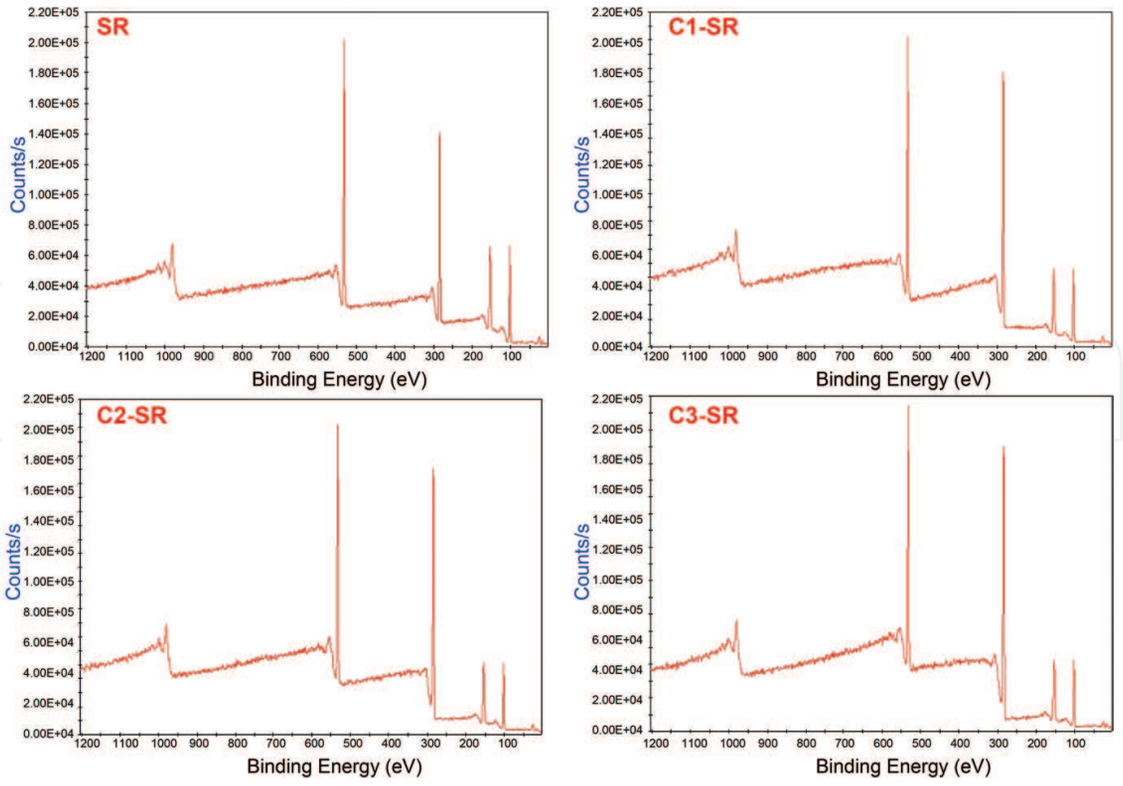

Figure 6. XPS results of virgin silicone rubber and carbon ion-implanted silicone rubber.

Group	Si 2p	C 1s	O 1s
SR	28.82	47.57	23.65
C1-SR	18.94	58.40	22.67
C2-SR	18.96	58.44	22.60
C3-SR	18.13	61.49	20.38

Table 1. Chemical composition (in at.%) from the XPS analysis.

that with the ion implantation dose increasing, the carbon content in the material increased, while the Si content decreased, suggesting that implanted carbon atom may replace the Si of virgin SR, interrupting the original Si-O assemble, increasing the surface free energy, and, thereby, theoretically decreasing material's water contact angle.

Furthermore, AFM images revealed that the surfaces of C-SRs were composed of larger irregular peaks and deeper valleys, while virgin SR exhibited a relatively smooth and more homogeneous surface (**Figure 7A**). The surface roughness of the C3-SR, which underwent most carbon ion implantation, was highest among all three C-SRs (**Figure 7B**).

In addition, all samples exhibited negative zeta potentials and reflect that the surfaces of all samples were negatively charged. The absolute value of the zeta potential increased with the ion dose (**Figure 8**). Considering the influence of surface roughness on contact angle, we propose that ion implantation can change the surface roughness of the material and increase the surface potential of the material.

3.2. Ion implantation inhibits bacterial adhesion on SR

Preventing bacterial adhesion and biofilm formation by improving the surface antibacterial adhesion property of the silicone rubber is critical for eliminating various types of infections.

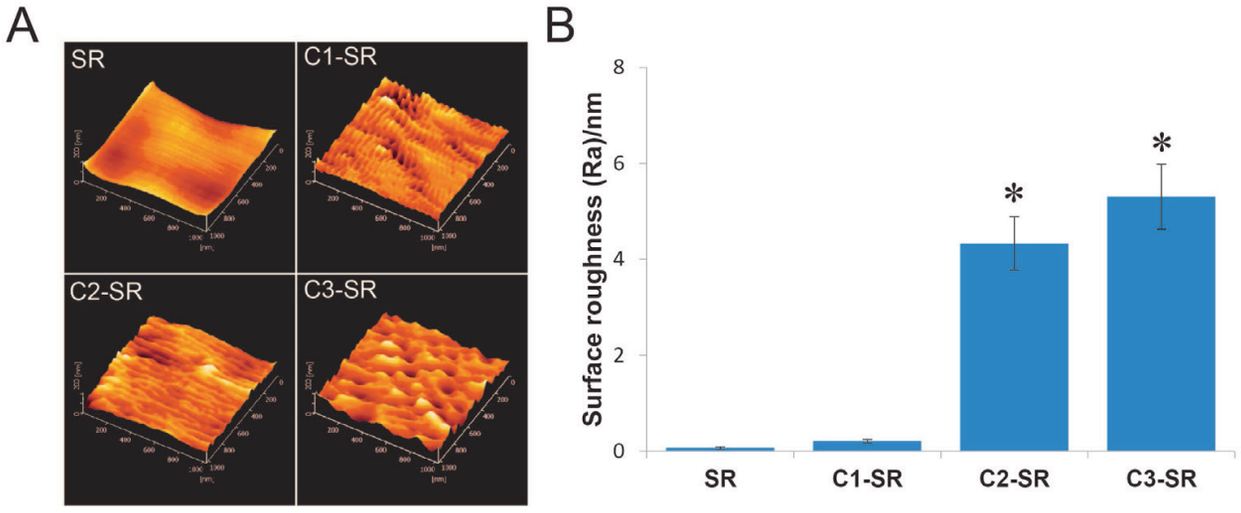

Figure 7. AFM results of virgin silicone rubber and carbon ion-implanted silicone rubber. A, Representative atomic force microscope images. B, Surface roughness (*P < 0.01 compared with silicone rubber).

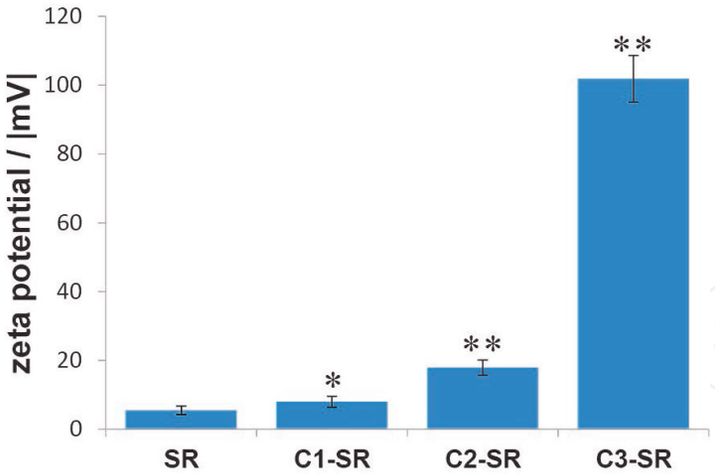

Figure 8. The zeta potential of virgin silicone rubber and carbon ion-implanted silicone rubber (*P < 0.05 compared with silicone rubber; **P < 0.01 compared with silicone rubber).

After ion implantation, we used Gram-negative *Escherichia coli* (American Type Culture Collection 25922) to evaluate the ability to resist bacteria adhesion. From the result, after 1 h of incubation, the rate of *E. coli* adherence on the carbon ion silicone rubber (1×10^{15} carbon ions/cm^2; 3×10^{15} carbon ions/cm^2; and 1×10^{16} carbon ions/cm^2) increased to approximately 11, 25, and 33%, respectively, and that on carbon ion silicone rubber increased significantly after 1 h of incubation (**Figure 9**) ($P < 0.05$).

After 24 h of incubation, the rates of bacterial adherence were slightly lower, but did not significantly decrease compared with that after 1 h of incubation ($P > 0.05$). The ability of carbon ion silicone rubber to prevent viable bacteria colonization was also verified by fluorescence staining. The results had shown that the amount of bacterial adhesion to the surface of carbon ion silicone rubber was reduced compared with the virgin silicone rubber (**Figure 10**). Scanning electron microscopy was performed to examine the attached bacteria. As the results

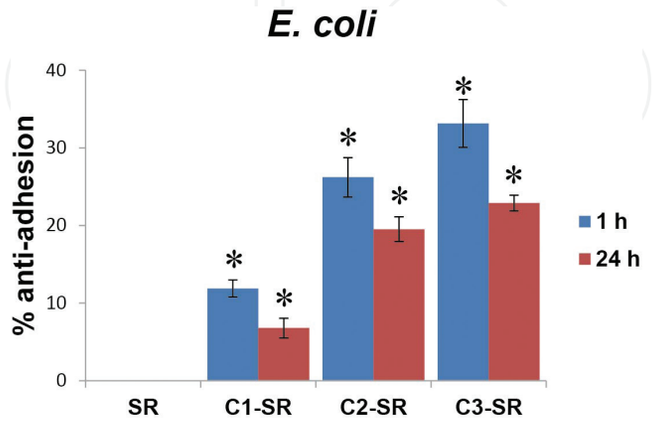

Figure 9. The antiadhesion rates (%) of virgin silicone rubber and carbon ion-implanted silicone rubber. After all samples were cultured in bacterial suspension for 1 and 24 h, bacteria on the surface of all samples were recultured on the plate, and bacterial colonies were subsequently counted. According to the number of colonies, the antiadhesion rates (%) for *E. coli* were calculated. The data are presented as the mean ± SD (n = 3); *$P < 0.05$ compared with silicone rubber.

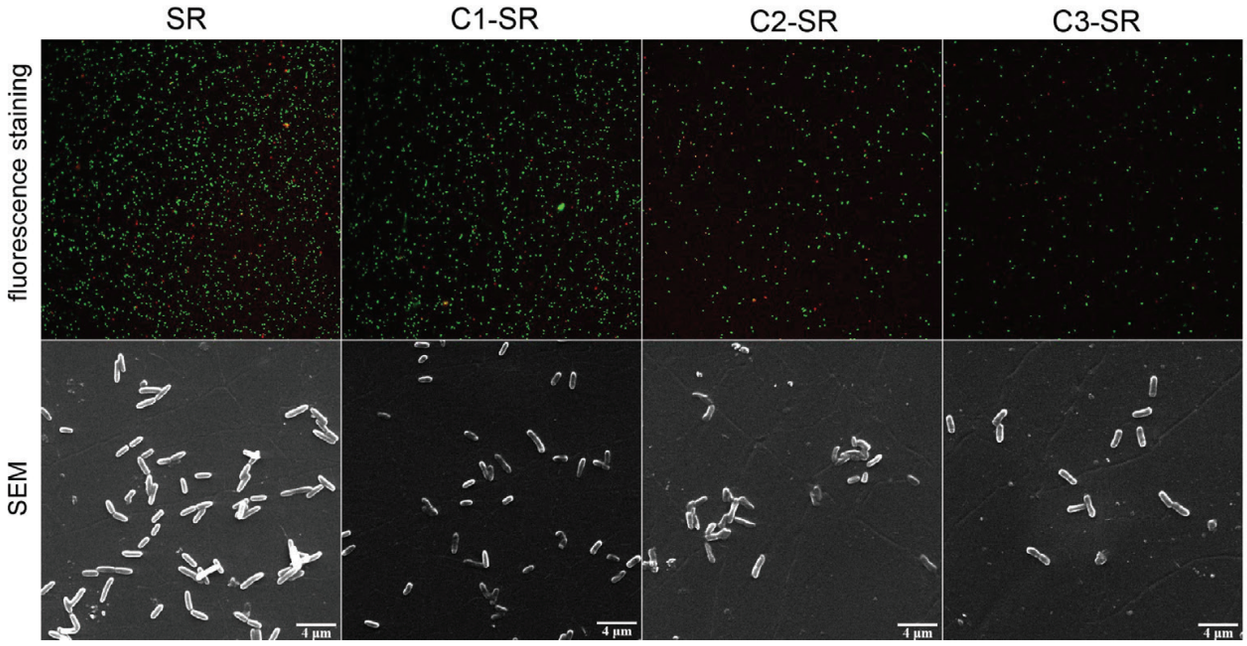

Figure 10. Representative images of fluorescence staining and scanning electron microscopy observation of virgin silicone rubber and carbon ion-implanted silicone rubber. Representative images showing bacteria viability on SR and CSR after 24 h of incubation, as indicated by staining with a LIVE/DEAD BacLight Bacterial Viability Kit (Thermo Fisher Scientific, Waltham, Mass). The live bacteria appear green, whereas the dead bacteria are red (original magnification, × 200). Representative scanning electron microscopic images of the bacteria on SR and CSR after incubation for 24 h.

have shown that bacteria were observed on surfaces of all samples, but there were differences in quantity (**Figure 10**).

3.3. Carbon ion-implanted silicone rubber triggers thinner and weaker tissue capsules

After ion implantation, the host responses were evaluated by surveying inflammation and fibber capsule formation that developed after subcutaneous implantation in Sprague-Dawley rats for 7, 30, 90, and 180 days. The thickness values of tissue capsules around the implants were identified from hematoxylin and eosin-stained sections of the peri-implant soft tissues and were analyzed as one of the physiologic responses to implantation. At 7 days after implantation, silicone rubber had the thinnest tissue capsules, and carbon ion silicone rubber had thicker (**Figure 11**) ($P > 0.05$) and weaker tissue capsules. Interestingly, the thickness decreased with longer implantation and increasing carbon ion doses (**Figure 11**). At 180 days after implantation, silicone rubber and C3-SR had the thickest and the thinnest tissue capsules, respectively (**Figure 11**).

In addition, collagen deposition was revealed using Masson trichrome staining. Our results show that collagen gradually became sparser over time and with increasing carbon ion doses. Carbon ion silicone rubber had obviously lower collagen deposition than silicone rubber (**Figure 12**) ($P < 0.05$).

To gain insight into inflammatory foreign body responses and capsule contracture to the samples, major biomarkers CD68, CD4, tumor necrosis factor-α, elastin, and α-smooth muscle

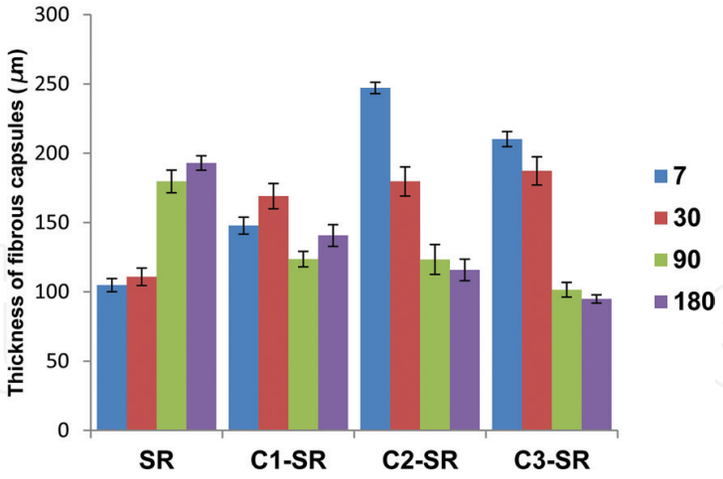

Figure 11. The capsule thicknesses around the implants.

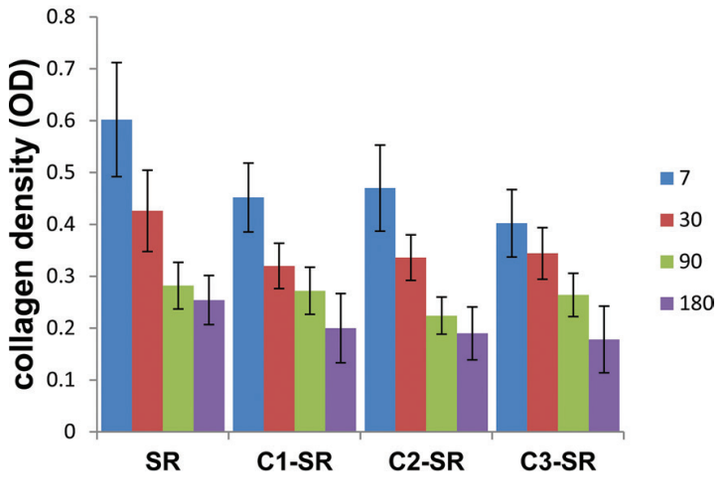

Figure 12. The collagen density around the implants.

actin were detected using immunohistochemistry. As shown in **Table 2**, all samples present lower expression of CD68, with no significant differences.

The distribution of CD4 in the inflammatory infiltrate, which was induced by the samples, was investigated to further understand the local immunomodulation against these types of materials. The results show that there were many positive staining areas of CD4 in silicone

	7 days	30 days	90 days	180 days
SR	+	+	+	+
C1-SR	+	+	+	+
C2-SR	+	+	+	+
C3-SR	+	+	+	+

Table 2. Semiquantitative evaluation of CD68 in peri-implant tissue.

rubber after 90 days, but positive staining in the carbon ion silicone rubber decreased with time. After 90 days, CD4 significantly decreased compared with silicone rubber (**Table 3**).

In addition, the expression results of proinflammatory cytokine tumor necrosis factor-α by macrophage cells show that silicone rubber had an obviously positive staining area (**Table 4**).

Furthermore, the positive staining areas of α-smooth muscle actin and elastin have no difference; the positive staining area of α-smooth muscle actin appeared predominantly in silicone rubber than in carbon ion silicone rubber (**Table 5**). Elastin was intensely expressed in silicone rubber, particularly after 30 days (**Table 6**).

	7 days	**30 days**	**90 days**	**180 days**
SR	++	++	+++	+++
C1-SR	+++	++	+	+
C2-SR	++	++	++	++
C3-SR	++	+	+	+

Table 3. Semiquantitative evaluation of CD4 in peri-implant tissue.

	7 days	**30 days**	**90 days**	**180 days**
SR	++	++	+++	+++
C1-SR	++	++	+	+
C2-SR	+++	+	+	+
C3-SR	++	+	+	+

Table 4. Semiquantitative evaluation of TNF-α in peri-implant tissue.

	7 days	**30 days**	**90 days**	**180 days**
SR	+	++	++	++
C1-SR	+	+	+	+
C2-SR	+	+	+	+
C3-SR	+	+	+	+

Table 5. Semiquantitative evaluation of α-SMA in peri-implant tissue.

	7 days	**30 days**	**90 days**	**180 days**
SR	++	+++	+++	++
C1-SR	+	++	++	+
C2-SR	++	+	++	+
C3-SR	++	++	+	+

Table 6. Semiquantitative evaluation of elastin in peri-implant tissue.

4. Conclusion

Our study evaluated the in vitro antibacterial properties and the in vivo host response to carbon ion-implanted silicone rubber. The results of our study indicate that the carbon ion silicone rubbers have good biocompatibility, lower bacterial adhesion, and lower foreign body reaction with relatively thin fibrous capsules. All results show that ion implantation should be considered for further investigation and application, and carbon ion silicone rubber might be a better biomaterial for decreasing silicone rubber-initiated complications.

Acknowledgements

This work was funded by grants from the National Natural Science Foundation of China (81571918, 81401610) and a grant for Scientific Personnel Innovation from Chongqing (cstc2013kjrc-qnrc10003).

Author details

Xin Zhou, Yiming Zhang, Xiaohua Shi and Dongli Fan*

*Address all correspondence to: fdltmmu@sina.com

Department of Plastic and Cosmetic Surgery, Xinqiao Hospital, Third Military Medical University, Chongqing, China

References

[1] Liu P, Chen Q, Yuan B, Chen M, Wu S, Lin S, Shen J. Facile surface modification of silicone rubber with zwitterionic polymers for improving blood compatibility. Materials Science & Engineering C-Materials for Biological Applications. 2013;**33**(7):3865-3874. DOI: 10.1016/j.msec.2013.05.025

[2] Lugowski SJ, Smith DC, Bonek H, Lugowski J, Peters W, Semple J. Analysis of silicon in human tissues with special reference to silicone breast implants. Journal of Trace Elements in Medicine and Biology. 2000;**14**(1):31-42. DOI: 10.1016/S0946-672X(00)80021-8

[3] Erlich MA, Parhiscar A. Nasal dorsal augmentation with silicone implants. Facial Plastic Surgery. 2003;**19**(4):325-330. DOI: 10.1055/s-2004-815652

[4] Cazacu M, Racles C, Vlad A, Antohe M, Forna N. Silicone-based composite for relining of removable dental prosthesis. Journal of Composite Materials. 2009;**43**(10):2045-2055. DOI: 10.1177/0021998309340447

[5] Anderson JM, Rodriguez A, Chang DT. Foreign body reaction to biomaterials. Seminars in Immunology. 2008;**20**(2):86-100. DOI: 10.1016/j.smim.2007.11.004

[6] Rohrich RJ. Advances in breast augmentation. Plastic and Reconstructive Surgery. 2006;**118**(7):1S-2S. DOI: 10.1097/01.prs.0000247292.96867.06

[7] Vasilev K, Cook J, Griesser HJ. Antibacterial surfaces for biomedical devices. Expert Review of Medical Devices. 2009;**6**(5):553-567. DOI: 10.1586/erd.09.36

[8] Bazaka K, Jacob MV, Crawford RJ, Ivanova EP. Plasma-assisted surface modification of organic biopolymers to prevent bacterial attachment. Acta Biomaterialia. 2011; **7**(5):2015-2028. DOI: 10.1016/j.actbio.2010.12.024

[9] Bergmann PA, Tamouridis G, Lohmeyer JA, Mauss KL, Becker B, Knobloch J, Mail Nder P, Siemers F. The effect of a bacterial contamination on the formation of capsular contracture with polyurethane breast implants in comparison with textured silicone implants: An animal study. Journal of Plastic Reconstructive and Aesthetic Surgery. 2014;**67**(10):1364-1370. DOI: 10.1016/j.bjps.2014.05.040

[10] Tang CY, Chen D-Z, Chan KYY, Chu KM, Ng PC, Yue TM. Fabrication of antibacterial silicone composite by an antibacterial agent deposition, solution casting and crosslinking technique. Polymer International. 2011;**60**(10):1461-1466. DOI: 10.1002/pi.3102

[11] Xue L, Zhang Y, Zuo Y, Diao S, Zhang J, Feng S. Preparation and characterization of novel UV-curing silicone rubber via thiol-ene reaction. Materials Letters. 2013;**106**:425-427. DOI: 10.1016/j.matlet.2013.05.084

[12] van der Houwen EB, Kuiper LH, Burgerhof JG, van der Laan BF, Verkerke GJ. Functional buckling behavior of silicone rubber shells for biomedical use. Journal of the Mechanical Behavior of Biomedical Materials. 2013;**28**:47-54. DOI: 10.1016/j.jmbbm.2013.07.002

[13] Abbasi F, Mirzadeh H, Katbab AA. Modification of polysiloxane polymers for biomedical applications: A review. Polymer International. 2001;**50**(12):1279-1287. DOI: 10.1002/pi.783

[14] Magennis EP, Hook AL, Williams P, Alexander MR. Making silicone rubber highly resistant to bacterial attachment using thiol-ene grafting. ACS Applied Materials & Interfaces. 2016;**8**(45):30780-30787. DOI: 10.1021/acsami.6b10986

[15] Ziraki S, Zebarjad SM, Hadianfard MJ. A study on the role of polypropylene fibers and silica nanoparticles on the compression properties of silicone rubber composites as a material of finger joint implant. International Journal of Polymeric Materials and Polymeric Biomaterials. 2017;**66**(1):48-52. DOI: 10.1080/00914037.2016.1180623

[16] Tsuji H, Izukawa M, Ikeguchi R, Kakinoki R, Sato H, Gotoh Y, Ishikawa J. Surface treatment of silicone rubber by carbon negative-ion implantation for nerve regeneration. Applied Surface Science. 2004;**235**(1–2):182-187. DOI: 10.1016/j.apsusc.2004.05.121

[17] Tsuji H, Sommani P, Hattori M, Yamada T, Sato H, Gotoh Y, Ishikawa J. Negative ion implantation for patterning mesenchymal-stem cell adhesion on silicone rubber and

differentiation into nerve cells with keeping their adhesion pattern. Surface and Coatings Technology. 2009;**2003**(17–18):2562-2565. DOI: 10.1016/j.surfcoat.2009.02.076

[18] Tsuji H, Sommani P, Kitamura T, Hattori M, Sato H, Gotoh Y, Ishikawa J. Nerve-cell attachment properties of polystyrene and silicone rubber modified by carbon negative-ionimplantation. Surface and Coatings Technology. 2007;**201**(19–10):8123-8126. DOI: 10.1016/j.surfcoat.2006.01.074

[19] Rahman CV, Ben-David D, Dhillon A, Kuhn G, Gould TWA, Muller R, Rose F, Shakesheff KM, Livne E. Controlled release of BMP-2 from a sintered polymer scaffold enhances bone repair in a mouse calvarial defect model. Journal of Tissue Engineering and Regenerative Medicine. 2014;**8**(1):59-66. DOI: 10.1002/term.1497

[20] Ling T, Lin J, Tu JJ, Liu SQ, Weng WJ, Cheng K, Wang HM, Du PY, Han GR. Mineralized collagen coatings formed by electrochemical deposition. Journal of Materials Science-Materials in Medicine. 2013;**24**(12):2709-2718. DOI: 10.1007/s10856-013-5028-9

[21] Meretoja VV, Rossi S, Peltola T, Pelliniemi LJ, Narhi TO. Adhesion and proliferation of human fibroblasts on sol–gel coated titania. Journal of Biomedical Materials Research Part A. 2010;**95A**(1):269-275. DOI: 10.1002/jbm.a.32829

[22] Baba K, Hatada R, Flege S, Ensinger W. Preparation and properties of Ag-containing diamond-like carbon films by magnetron plasma source ion implantation. Advances in Materials Science and Engineering. 2012;536853. DOI: 10.1155/2012/536853

[23] Dudognon J, Vayer M, Pineau A, Erre R. Mo and Ag ion implantation in austenitic, ferritic and duplex stainless steels: A comparative study. Surface and Coatings Technology. 2008;**203**(1–2):180-185. DOI: 10.1016/j.surfcoat.2008.08.069

[24] Fang J, Zhao JH, Sun Y, Ma HY, Yu XL, Ma Y, Ni YX, Zheng L, Zhou YM. Biocompatibility and antibacterial properties of zinc-ion implantation on titanium. Journal of Hard Tissue Biology. 2014;**23**(1):35-43.

[25] Hou XG, Wang XM, Luan WJ, Li DJ, Dong L, Ma J. Study of antibacterial, hydrophilic and nanomechanical properties of TiOx films modified by Ag+ beam implantation. Surface and Coatings Technology. 2013;**229**:71-75. DOI: 10.1016/j.surfcoat.2012.04.092

IntechOpen